Semiconducting chalcogenide buffer layer for oxide heteroepitaxy on Si(001)

D. A. Schmidt[a)]
Department of Physics University of Washington (UW), Seattle, Washington 98195-1560 and Center for Nanotechnology (CNT), University of Washington (UW), Seattle, Washington 98195-1560

Taisuke Ohta[b)] and C.-Y. Lu
Department of Materials Science and Engineering, UW, Seattle, Washington 98195-2120 and CNT, UW, Seattle, Washington 98195-2120

Aaron A. Bostwick[b)] and Q. Yu[c)]
Department of Physics, UW, Seattle, Washington 98195-1560

Eli Rotenberg
Advanced Light Source, Berkeley, California 94720

F. S. Ohuchi
Department of Materials Science and Engineering, UW, Seattle, Washington 98195-2120 and CNT, UW, Seattle, Washington 98195-2120

Marjorie A. Olmstead
Department of Physics, UW, Seattle, Washington 98195-1560 and CNT, UW, Seattle, Washington 98195-1560

(Received 9 December 2005; accepted 12 March 2006; published online 2 May 2006)

We report controlled laminar growth of a crystalline transition metal oxide on Si(001) *without* SiO_x or silicide formation by utilizing the chalcogenide semiconductor gallium sesquiselenide (Ga_2Se_3) as a nonreactive buffer layer. Initial nucleation of both pure and Co-doped anatase (TiO_2) is along Ga_2Se_3 nanowire structures, coalescing to a flat, multidomain film within two molecular layers. Arsenic-terminated Si(001) [Si(001):As] is stable against pure O_2, but oxidizes when both Ti and O_2 are present. The Si–TiO_2 valence band offset using either buffer layer is about 2.8 eV, producing a staggered band alignment. © *2006 American Institute of Physics*. [DOI: 10.1063/1.2199451]

Integration of crystalline oxides with silicon is a critical component of myriad proposed applications, including spintronic,[1,2] ferroelectric, and ferroic devices.[3] Anatase-structure TiO_2, which is nearly lattice matched to Si, shows particular promise for Si-based nanoelectronics[4] and, when doped with Co or Cr, spintronics.[5,6] However, full integration of crystalline-oxide-based functionalities into Si technology is currently impeded by spontaneous formation of amorphous oxides and/or silicides at the Si/oxide interface.

Subnanometer buffer layers can prevent interface reactions while preserving oxide functionality. Most notable among current buffers is a Sr–O interlayer for $SrTiO_3$ heteroepitaxy on Si(001),[7,8] although substrate oxidation can occur during subsequent TiO_2 deposition.[9] Ultrathin SiO_2 has been utilized for TiO_2 growth, resulting in an amorphous titanium silicate interface layer.[10] An amorphous high band gap interlayer is acceptable for gate-insulator applications, but not for ferroelectric or ferromagnetic applications requiring crystalline oxides and/or nonscattering interfaces.

Here, we demonstrate a chalcogenide-based buffer layer, Ga_2Se_3/As, for laminar heteroepitaxy of both pure and cobalt-doped (5%) anatase (Co:TiO_2). Co:TiO_2 is known to be ferromagnetic at room temperature;[5,6] Ga_2Se_3 has a band gap of 2.1 eV,[11,12] between those of Si and TiO_2 (1.1 and 3.2 eV, respectively), and nearly the same lattice constant.[13] Ga_2Se_3 forms a stable, epitaxial, nonreactive layer on Si(001):As.[14] The intrinsic vacancy structure of β-Ga_2Se_3, with one-third of the cation sites vacant in a zinc blende structure, also enables flexible strain relief. We observe neither oxide nor silicide formation at the buried Si interface, nor any buffer layer reactions; we also find a staggered band alignment, enabling electron transport from Si to TiO_2, but not vice versa. No evidence is found for the Co-rich surface clusters reported[9,15,16] with other growth methods. We also investigated Si(001):As as a buffer layer; it is stable in pure O_2 but allows oxidation of Si in the presence of Ti.

TiO_2 and Co:TiO_2 films and the As and Ga_2Se_3 buffer layers were deposited on clean *p*-type Si(001) ($\rho = 0.02–0.1\ \Omega$ cm) by molecular beam epitaxy and characterized *in situ* by scanning tunneling microscopy (STM), photoemission spectroscopy (PES), and x-ray absorption near-edge structure (XANES). Buffer layers were deposited as by Ohta *et al.*,[14] first terminating the Si(001) surface with one monolayer of As and then adding ~0.8 nm Ga_2Se_3. Pure Ti or a Co:Ti alloy rod (95% Ti, 5% Co) was heated with an electron beam in an oxygen background ($P_{O_2} = 5 \times 10^{-5}$ Torr) to deposit TiO_2 or Co:TiO_2 at either room or elevated (350–400 °C) temperature. XANES measurements showed films grown at either room temperature (RT) or 350 °C to have a Ti *L*-edge structure consistent with anatase standards grown on $LaAlO_3$(001), and inconsistent with rutile. Higher temperature deposition (500–600 °C) results in growth of rutile nanocrystals; still higher destroys the buffer layer and oxidizes the substrate.[17]

[a)]Present address: International Center for Young Scientists, NIMS, Tsukuba, Japan.
[b)]Present address: Advanced Light Source, Berkeley, CA 94720.
[c)]Present address: CNT, UW, Seattle, WA 98195-2140.

0003-6951/2006/88(18)/181903/3/$23.00

© 2006 American Institute of Physics
Downloaded 08 Jul 2010 to 128.95.93.90. Redistribution subject to AIP license or copyright; see http://apl.aip.org/apl/copyright.jsp

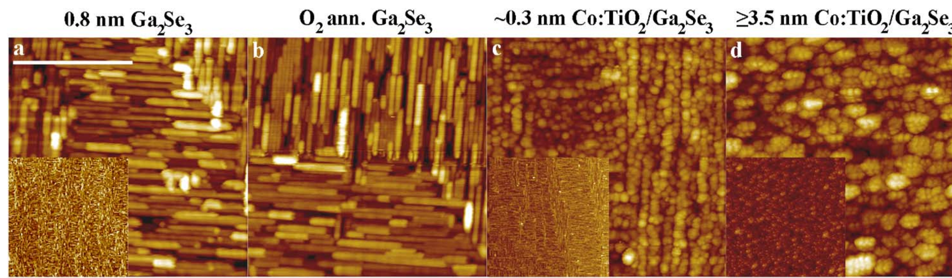

FIG. 1. (Color online) Surface morphology of buffer layers and oxide film. 100×100 nm^2 STM images (500×500 nm^2 insets): (a) $\sim$0.8 nm Ga_2Se_3; (b) O_2 (P_{O_2} $\sim5\times10^{-5}$ Torr) annealed (T_{ann}=450 °C) Ga_2Se_3; (c) $\sim$0.3 nm Co:TiO_2 film on $\sim$0.8 nm Ga_2Se_3; (d) $\geq$3.5 nm Co:TiO_2 film on $\sim$0.8 nm Ga_2Se_3. Scale bar in (a) is 50 nm. Nanoridges are in [110] directions and differ in height by 0.27 nm. Image conditions: (a) 2.5 V, 0.07 nA, inset: −4.5 V, 0.09 nA; (b) 2.8 V, 0.1 nA; (c) 2.8 V, 0.09 nA, inset: 2.8 V, 0.09 nA; (d) 2 V, 0.12 nA, inset: 2.9 V, 0.1 nA.

The Ga_2Se_3 buffer layer self-assembles into oriented nanoridges, tens of nanometers long and 1–2 nm wide at their base [Fig. 1(a)], generated by ordered surface coalescence of intrinsic vacancies. The Ga-topped ridges have (111) Se facets and change direction at each substrate step.[14,18] This morphology is stable against oxidation in $P_{O_2}=5\times10^{-5}$ Torr at 450 °C [compare Figs. 1(a) and 1(b)]. PES shows no oxygen accumulation (within an experimental sensitivity of $\lesssim$2% of a monolayer). The observed narrowing, smoothing, and aligning of the nanoridge morphology also occurs during an equivalent anneal without O_2 ($P_{tot}\leq1\times10^{-10}$ Torr). The root-mean-square (rms) surface roughness over 1.0 μm^2 is 0.24 nm, comparable to that of bare Si(001) (see Table I). On a smaller scale [Fig. 2(a), 30×50 nm^2], six nanoridge levels (0.27 nm height difference) are exposed on what was originally two Si terraces.

RT deposition of about 1 ML (molecular layer) Co:TiO_2 on this Ga_2Se_3/As buffer layer nucleates as 1 ML high clusters with centers spaced by 2–3 nm along the Ga_2Se_3 nanoridges [Fig. 1(c)]. The large-scale nanoridge morphology is unchanged (Fig. 1 insets). The first 1–2 ML have comparable roughness to the starting buffer layer (Table I). Deposition at 350 °C [Fig. 2(c)] produces comparable morphologies, although the higher temperature (faster diffusion) growth leads to a larger spacing (3–4 nm) between the clusters. At coverages just below 1 ML, some underlying Ga_2Se_3 nanorods may be seen [e.g, x=14–18 nm in Figs. 2(f) and 2(c)], and sub-ML modulation is apparent on some larger islands.

Continued growth of Co:TiO_2 at either RT or 350 °C results in laminar films without large surface clusters [inset, Fig. 1(d)]. By 15–20 ML, the rms roughness of films grown at 350 °C has increased by only $\sim$1/3 ML (Table I); the film exhibits predominantly single ML height steps surrounding 5–10 nm diameter, kidney-bean shaped domains [Fig. 2(e)].

TABLE I. Z-range rms roughness (nm) as a function of preparation and scan size. For anatase films, Co:TiO_2 values in roman and TiO_2 in *italics*; deposition at RT, with T_{dep}=350 °C in parentheses.

Scan Range (μm^2)	Bare Si(001)	Si(001):As	$\sim$0.8 nm Ga_2Se_3	$\sim$0.3 nm Co:TiO_2 TiO_2	$\geq$3.5 nm Co:TiO_2 TiO_2
1.0×1.0	0.26	0.14	0.24	0.21	0.32
				0.27 (0.29)	0.36
0.5×0.5	0.19	0.10	0.23	*0.29* (*0.28*)	*0.40* (*0.34*)
				0.28 (0.24)	0.35
0.1×0.1	0.06	0.07	0.29	*0.28* (*0.26*)	*0.43* (*0.35*)

RT-deposited films are rougher, with 7–10 nm diameter islands, 3–4 ML high [Figs. 2(d) and 1(d)].

Bright dots of apparent height of 0.1 nm, spaced by $\sim$4–6 surface unit cells, are seen in the positive tip bias, filled-state images of T_{dep}=350 °C Co:TiO_2 films [Fig. 2(e)]. Their spacing matches the expected distance between uniformly distributed Co atoms, which comprised 5% of the source metal. Similar bright spots, though with higher density and concentrated at step edges, were reported for STM of Co:TiO_2 films on $SrTiO_3$,[19] where they were attributed to isolated Co atoms that remained after clusters dissolved upon annealing. In bulk Co:TiO_2, Co^{2+} substitution for Ti^{4+} likely has an associated O vacancy; a bright spot in occupied state images indicates enhanced negative charge, consistent with an intact O lattice near a surface Co^{2+} impurity. The local morphology of pure TiO_2 films (not shown) is indistinguishable from Co:TiO_2 except for these bright dots.

Chemical reactions at the buried Si–buffer layer interface were investigated with photoemission spectroscopy (PES) at the Advanced Light Source (Beamline 7.0.1). Both Si(001):As and Ga_2Se_3 buffer layers are inert in partial pressures of O_2 ($P_{O_2}=5\times10^{-5}$ Torr) and $T_{ann}\leq500$ °C. High resolution, surface-sensitive, core-level spectroscopy (Fig. 3) reveals no oxidized Si component for either Ga_2Se_3 or Si(001):As. In the presence of both Ti and O_2, a significant oxidized Si 2p component is observed for Si(001):As (peak at 102 eV in Fig. 3), indicating that Ti catalyzes the Si–O reaction. The As 3d (not shown) also shows a reacted component upon TiO_2 deposition. TiO_2 growth on Ga_2Se_3/Si(001):As, however, shows no reacted substrate components. As the TiO_2 film grows thicker, all substrate peaks attenuate exponentially and show no additional components, as expected for a nonreactive, laminar deposition.[17]

We propose that TiO_2 nuclei react with Se-terminated sides or valleys between the nanoridges. Ga–Ti interactions would lead to metallic states in PES, while Ga–O reactions would cause a new Ga 3d component; neither were observed. Interface Ti–Se interactions may not have a clear PES signature. Se atoms can effectively "oxidize" the Ti adatoms and stabilize them at the surface for reaction with incident O_2. No O adsorbs without Ti present. For Si(001):As, Ti likely rests in trenches between As dimer rows, weakening Si–As bonds to promote Si oxidation. The larger bond enthalpy of Si–O relative to Ti–O leads to preferential bonding to Si.

A key parameter for device applications of TiO_2/Si is the band alignment. Figure 3 shows valence band (VB) emission, highlighted with lines marking the band edges, using the known energy difference[20] between our measured Si 2p

Downloaded 08 Jul 2010 to 128.95.93.90. Redistribution subject to AIP license or copyright; see http://apl.aip.org/apl/copyright.jsp

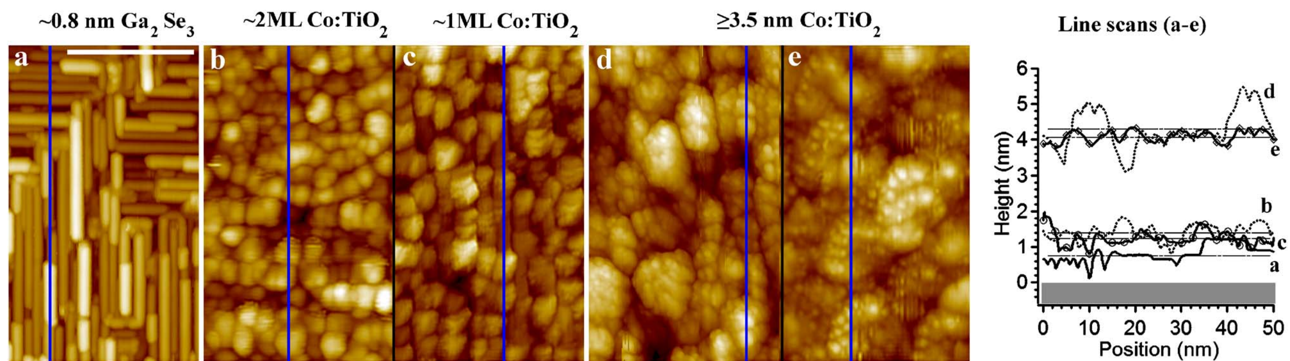

FIG. 2. (Color online) High resolution surface morphology of buffer layer and oxide films. 30×50 nm^2 STM images of (a) ~0.8 nm Ga_2Se_3; (b)–(e) Co:TiO_2 films on ~0.8 nm Ga_2Se_3: (b) ~0.2 nm (2 ML), T_{dep}=RT; (c) ~0.08 nm (1 ML), T_{dep}=350 °C; (d) ⩾3.5 nm (20 ML), T_{dep}=RT; (e) ⩾3.5 nm (20 ML), T_{dep}=350 °C; (f) cross-sectional line scans [110] (vertical lines) from (a)–(e). (a) Solid line, (b) dotted line, (c) solid+circles, (d) dotted line, and (e) solid +diamonds. Scale bar in (a) is 20 nm. Image conditions: (a) −5.4 V, 0.09 nA; [(b) and (c)] 2.8 V, 0.09 nA; (d) 1.8 V, 0.09 nA; (e) 3.6 V, 0.1 nA.

or Ti 3*p* emission and the respective VB maximum, and band gaps of 3.2 eV for anatase and 1.1 eV for Si. The VB offset (VBO) is 2.77±0.1 eV for the Ga_2Se_3 buffer layer and 2.86±0.1 eV for As alone. These are well above the VBO values of 1.65–2.55 eV for TiO_2 on a SiO_2 buffer layer,[10] 1.93 eV for SrO/$SrTiO_2$ buffers,[20] and 2.0 eV predicted from charge neutrality level alignment.[21] This indicates a significant interface dipole contribution from the As and Ga_2Se_3 buffer layers, possibly including As interdiffusion. It should therefore be possible to shift this alignment through the manipulation of interface dipoles. Our measured VBO identifies a staggered band alignment, with the anatase conduction band minimum about 0.7 eV below of that of Si; this allows electron transport from Si to TiO_2, but forms a barrier in the other direction.

In summary, we presented heteroepitaxy of laminar TiO_2 and Co:TiO_2 on Si(001) without reactions at the buried silicon interface through the use of Ga_2Se_3 as a buffer layer. The oxide nucleates between Ga_2Se_3 nanoridges, with further growth leading to laminar films with low surface roughness. No segregated particles are observed. We do not find successful oxide heteroepitaxy on As-terminated silicon. Finally, we find a staggered band alignment between the TiO_2 film and the Si substrate. We believe that Ga_2Se_3 films may be extended for use as a buffer layer with other oxide heteroepitaxial systems.

This work was supported by NSF Grant No. ECS 0224138 and M. J. Murdock Charitable Trust. One of the authors (D.A.S.) acknowledges support from the UW-PNNL Joint Institute for Nanoscience and another author (T.O.) from the UW-CNT University Initiative Fund. Some data were obtained at the Advanced Light Source (Berkeley, CA; DOE Contract No. DE-AC03-76SF00098). The authors thank S. A. Chambers for fruitful discussions and for epitaxial anatase and rutile standards. Portions of this work were submitted by one of the authors (D.A.S.) in partial fulfillment of the requirements for the Ph.D. at UW.

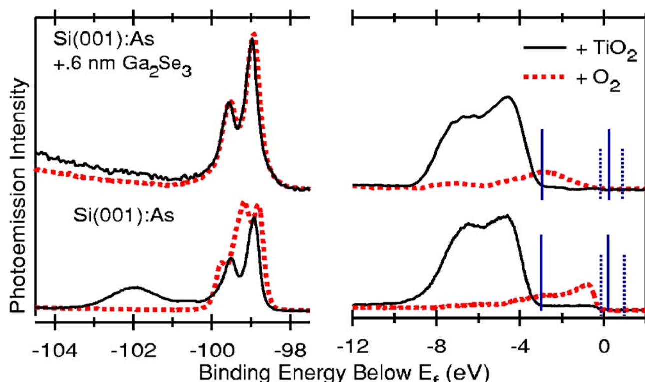

FIG. 3. (Color online) Chemical passivity of buffer layer. Si 2*p* (left) and valence band (right) normal emission photoelectron spectra for Si(001):As (bottom) and Si(001):As+0.6 nm Ga_2Se_3 (top) plus O_2 (dotted curve) or ~0.5 nm TiO_2 film (solid curve). Photon energy, $h\nu$=160 eV. Si 2*p* peak intensities scaled to the same area. Vertical lines show location of VBM and CBM for TiO_2 (solid) and Si (dotted) (see text).

[1] S. A. Wolf, D. D. Awschalom, R. A. Buhrman, and J. M. Daughton, Science **294**, 1488 (2001).
[2] D. D. Awschalom, M. B. Flatte, and N. Samarth, Sci. Am. **286**, 66 (2002).
[3] J. B. Goodenough, Rep. Prog. Phys. **67**, 1915 (2004).
[4] S. A. Campbell, H.-S. Kim, D. C. Gilmer, B. He, T. Ma, and W. L. Gladfelter, IBM J. Res. Dev. **43**, 383 (1999).
[5] Y. Matsumoto, M. Murakami, M. Shono, T. Hasegawa, T. Fukumura, M. Kawasaki, P. Ahmet, T. Chikyow, S. Koshihara, and H. Koinuma, Science **291**, 854 (2001).
[6] S. A. Chambers, S. Thevuthasan, R. F. C. Farrow, R. F. Marks, J. U. Thiele, L. Folks, M. G. Samant, A. J. Kellock, N. Ruzycki, D. L. Ederer, and U. Diebold, Appl. Phys. Lett. **79**, 3467 (2001).
[7] R. A. McKee, F. J. Walker, and M. F. Chisholm, Phys. Rev. Lett. **81**, 3014 (1998).
[8] R. A. McKee, F. J. Walker, M. B. Nardelli, W. A. Shelton, and G. M. Stocks, Science **300**, 1726 (2003).
[9] T. C. Kaspar, T. Droubay, C. M. Wang, S. M. Heald, A. S. Lea, and S. A. Chambers, J. Appl. Phys. **97**, 073511 (2005).
[10] C. C. Fulton, G. Lucovsky, and R. J. Nemanich, Appl. Phys. Lett. **84**, 580 (2004).
[11] C.-S. Yoon, K.-H. Park, D.-T. Kim, T.-Y. Park, M.-S. Jin, S.-K. Oh, and W.-T. Kim, J. Phys. Chem. **62**, 1131 (2001).
[12] S. Morley, M. von-der-Emde, D. R. T. Zahn, V. Offermann, T. L. Ng, N. Maung, A. C. Wright, G. H. Fan, I. B. Poole, and J. O. Williams, J. Appl. Phys. **79**, 3196 (1996).
[13] The unreconstructed (001) surface lattice parameters for β-Ga_2Se_3, Si, and anatase TiO_2 are a_s=0.382, 0.383, and 0.379 nm, respectively. The (001) step heights are multiples of 0.274, 0.136, and 0.24 nm for Ga_2Se_3, Si, and anatase, respectively.
[14] Taisuke Ohta, D. A. Schmidt, Shuang Meng, A. Klust, Q. Yu, M. A. Olmstead, and F. S. Ohuchi, Phys. Rev. Lett. **94**, 116102 (2005).
[15] S. A. Chambers, T. Droubay, C. M. Wang, A. S. Lea, R. F. C. Farrow, L. Folks, V. Deline, and S. Anders, Appl. Phys. Lett. **82**, 1257 (2003).
[16] J.-Y. Kim, J.-H. Park, B.-G. Park, H.-J. Noh, S.-J. Oh, J. S. Yang, D.-H. Kim, S. D. Bu, T.-W. Noh, H.-J. Lin, H.-H. Hsieh, and C. T. Chen, Phys. Rev. Lett. **90**, 017401 (2003).
[17] D. A. Schmidt, Ph.D. thesis, University of Washington, 2005.
[18] T. Ohta, Ph.D. thesis, University of Washington, 2004.
[19] J. S. Yang, D. H. Kim, S. D. Bu, T. W. Noh, S. H. Phark, Z. G. Khim, I. W. Lyo, and S.-J. Oh, Appl. Phys. Lett. **82**, 3080 (2003).
[20] A. C. Tuan, T. C. Kaspar, T. Droubay, J. W. Rogers, Jr., and S. A. Chambers, Appl. Phys. Lett. **83**, 3734 (2003).
[21] J. Robertson, J. Vac. Sci. Technol. B **18**, 1785 (2000).

Downloaded 08 Jul 2010 to 128.95.93.90. Redistribution subject to AIP license or copyright; see http://apl.aip.org/apl/copyright.jsp